Title

Planktonic biomass size spectra: An emergent property of size-dependent physiological rates, food web dynamics, and nutrient regimes

Journal

Marine Ecology Progress Series, 514

ISSN

0171-8630

Authors

Taniguchi, DAA
Franks, PJS
Poulin, FJ

Publication Date

2014

DOI

10.3354/meps10968

Peer reviewed

Vol. 514: 13–33, 2014
doi: 10.3354/meps10968

MARINE ECOLOGY PROGRESS SERIES
Mar Ecol Prog Ser

Published November 6

Planktonic biomass size spectra: an emergent property of size-dependent physiological rates, food web dynamics, and nutrient regimes

Darcy A. A. Taniguchi[1,3,*], Peter J. S. Franks[1], Francis J. Poulin[2]

[1]Scripps Institution of Oceanography, University of California, San Diego, La Jolla, California 92093-0208, USA
[2]Department of Applied Mathematics, University of Waterloo, Waterloo, Ontario, N2L 3G1, Canada

[3]*Present address:* Massachusetts Institute of Technology, Cambridge, Massachusetts 02142, USA

ABSTRACT: The systematic change in a trait with size is a concise means of representing the diversity and organization of planktonic organisms. Using this simplifying principle, we investigated how interactions between trophic levels, resource concentration, and physiological rates structure the planktonic community. Specifically, we used 3 size-structured nutrient-phytoplankton-zooplankton models differing in their trophic interactions, ranging from herbivorous grazing on one size class to omnivorous grazing on multiple size classes. We parameterized our models based on an extensive review of the literature. The maximum phytoplankton growth, maximum microzooplankton grazing, and phytoplankton half-saturation constant were found to vary inversely with size, and the nutrient half-saturation constant scaled positively with size. We examined the emergent community structure in our models under 4 nutrient regimes: 10, 20, 25, and 30 µM total N. In all models under all nutrient conditions, the normalized biomass of both phytoplankton and microzooplankton decreased with increasing size. As nutrients were increased, phytoplankton biomass was added to larger size classes with little change in the extant smaller size classes; for microzooplankton, spectra elongated and biomass was added to all size classes. The different grazing behaviors among models led to more subtle changes in the community structure. Overall, we found that phytoplankton are top-down controlled and microzooplankton are largely bottom-up controlled. Sensitivity analyses showed that both phytoplankton and microzooplankton biomass vary strongly with the size-dependence of the maximum grazing rate. Therefore, this parameter must be known with the greatest accuracy, given its large influence on the emergent community spectra.

KEY WORDS: Phytoplankton · Microzooplankton · Planktonic size spectra · Nutrient-phytoplankton-zooplankton models

INTRODUCTION

Planktonic communities are comprised of a wide variety of taxonomic and functional groups. Despite the diversity of these assemblages, the relative biomass and abundances of different sized organisms often scale systematically with size, with larger organisms generally less abundant than smaller organisms (e.g. Rodriguez & Mullin 1986, Chisholm 1992, Cavender-Bares et al. 2001, Reul et al. 2008). This size regularity influences the energy available for higher trophic levels, as trophic interactions are largely based on size (Sheldon et al. 1977, Hansen et al. 1994, Finkel 2007). The structure of planktonic size distributions is also relevant to biogeochemical cycling because sinking and nutrient uptake rates, for example, tend to scale with size (Moloney & Field 1991, Litchman et al. 2007, Edwards et al. 2012).

*Corresponding author: datanigu@mit.edu

Despite the importance of size in the ocean, it is not always clear what specific processes underlie the size structuring of natural communities.

The size-dependency of traits is called allometry. In its most general usage, allometry refers to the systematic change in a property with size (Gould 1966). More strictly, particularly among biologists, allometry refers to a trait's change with size according to the equation

$$c = as^b \quad (1)$$

where c is the trait, a is the scaling coefficient, s is a measure of size, and b is the scaling exponent not equal to 1 (which, strictly speaking, would refer to isometry).

The regular change in a planktonic property with size has been applied from early on to understand the distribution of planktonic community abundance (Sheldon et al. 1972). In the allometric scaling of plankton, there is generally a decrease in abundance or biomass with increasing size (larger plankton are relatively less abundant than smaller plankton; Fig. 1). When put in terms of Eq. (1), this relationship produces a negative b value (e.g. Platt & Denman 1978, Rodriguez & Mullin 1986, Reul et al. 2005). The lower the magnitude of b, the higher the proportion of larger plankton compared to smaller plankton.

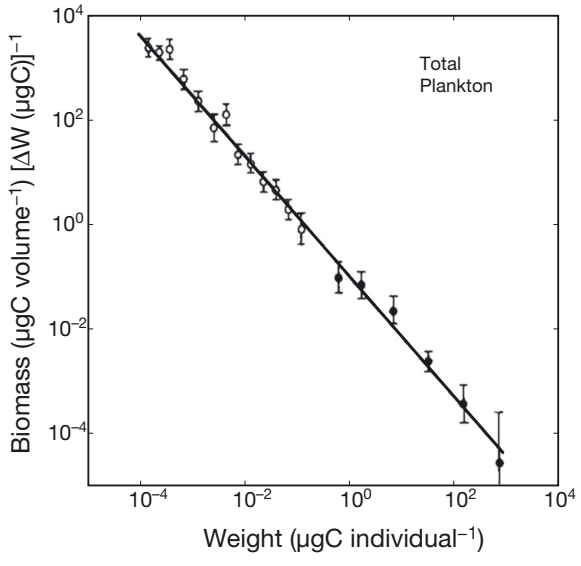

Fig. 1. Example of normalized planktonic biomass spectrum (Fig. 1 of Rodriguez & Mullin 1986), illustrating the decrease in biomass with increasing size (here based on weight). Data were collected from the North Pacific Central Gyre. The open symbols are for microplankton, the closed symbols for macroplankton, and the bars represent ±1 SD. Copyright 2014 by the Association for the Sciences of Limnology and Oceanography

The scaling coefficient a takes on a variety of values, depending on the units of the dependent variable, and provides a way to compare the absolute abundance or biomass of organisms with 1 unit of size (e.g. 1 µm^3). The size-abundance spectrum can change for a variety of reasons associated with temporal shifts such as seasonal and diel variability (Rodriguez & Mullin 1986) and with space, both vertically (Gin et al. 1999, Franks & Jaffe 2008) and horizontally (Reul et al. 2005).

To explain the variation in biomass with size, early theoretical models applied allometric relationships to planktonic rates (Kerr 1974, Platt & Denman 1977, 1978). Since then, a variety of empirically based allometric relationships have been discovered for a diverse suite of planktonic organisms and rates. While there are also several counterexamples in the literature (see 'Results and discussion'), the extent and variety of allometrically scaled rates remains noteworthy. For example, maximal growth rates for both phytoplankton (Banse 1976, Mizuno 1991, Edwards et al. 2012) and zooplankton (Hansen et al. 1997) show allometric scaling. Respiration (Fenchel & Finlay 1983, Tang & Peters 1995), photosynthesis (Finkel & Irwin 2000, Finkel et al. 2004, Marañón et al. 2007), and half-saturation constants for nutrient uptake (Eppley et al. 1969, Litchman et al. 2007) also show a systematic variation with size.

Allometric scalings of rates have been used to model processes from the detailed dynamics of plankton physiology and interactions (Steele & Frost 1977) all the way up to modeling entire global ecosystems (Ward et al. 2012). The usefulness of these allometric scalings for model parameterization lies in the relatively simple relationships. That is, allometric scalings allow the parameter values for all organisms, or at least distinct functional groups, to be reproduced using only 2 parameters, a and b. These allometric relationships simplify models while still maintaining diversity among organism types, based on size.

In this study, we take a detailed look at the size dependence of planktonic rates and how they interact with feeding behavior and ambient nutrient concentration to influence planktonic size distributions. In particular, we focused on the question: how do physiological, trophic, and environmental factors shape the emergent size structure of planktonic communities? To address this question, we used the framework of 3 size-structured nutrient-phytoplankton-zooplankton (NPZ) models with varying feeding connectivity. We used a synthesis of literature values to determine the size dependence of several physiological rates to parameterize these models. In partic-

ular, because of their importance in the marine food-web (Calbet & Landry 2004), we specifically examined the allometric relationships of microzooplankton and phytoplankton rates. Using those rates, we examined the emergent planktonic size distributions under different nutrient regimes in each of the 3 models. Finally, through a rigorous sensitivity analysis, we determined how influential each parameter is in determining the phytoplankton and zooplankton biomass and how each of those rate parameters combine to shape the emergent planktonic size spectra. This work elucidated the systematic change in rates with size and helped identify the dynamics that lead to regular biomass-size distributions in the oceans.

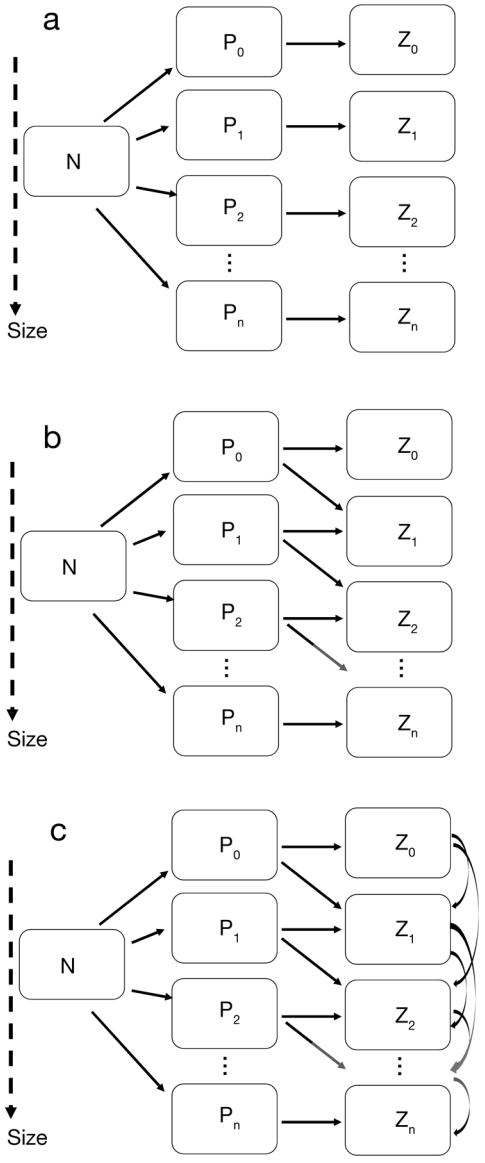

Fig. 2. Schematic representations of the 3 size structured nutrient-phytoplankton-zooplankton (NPZ) models. In each model, N represents dissolved nitrogen, P is phytoplankton, and Z is zooplankton. (a) Model 1: herbivorous grazing on one size class, (b) Model 2: herbivorous grazing on multiple size classes of phytoplankton, and (c) Model 3: omnivorous grazing on multiple size classes of phytoplankton and zooplankton. For clarity in depicting Models 2 and 3, we have only shown grazing on up to 2 size classes of plankton. In all models, we have not included the recycling arrows that show the contribution of phytoplankton and zooplankton to the dissolved nitrogen. The grayed arrow parts represent interactions with size classes not explicitly shown

Size-structured models

Our study aims to develop an accurate parameterization of 3 size-structured nutrient-phytoplankton-zooplankton (NPZ) models of increasing trophic complexity. By using updated planktonic parameterizations in each of the 3 models, we can make more significant, scientifically relevant comparisons of the influence of trophic dynamics in each of the 3 models. The base model is that of Poulin & Franks (2010). Although the model is described in detail in its original publication, we will describe it briefly here and clarify some differences between our parameterization and that of the original. We also describe 2 other models for which it is a foundation.

The 3 models we used are referred to as follows: Model 1, herbivorous grazers eating only one size class of phytoplankton; Model 2, herbivorous grazers eating multiple size classes of phytoplankton; and Model 3, omnivorous predators eating multiple size classes of (potentially) both phytoplankton and zooplankton (Fig. 2). While the 3 models differ in very fundamental ways, they share a similar framework. All 3 size-structured NPZ models are described by the equations

$$N_T = N + \sum_{i=1}^{n} P(s_i) + \sum_{i=1}^{n} Z(s_i) \quad (2)$$

$$\frac{\mathrm{d}P(s)}{\mathrm{d}t} = P(s)\left[\mu(s)\frac{N}{N+k_s(s)} - \Lambda(s) - \alpha g(rs)\frac{Z(rs)}{F(s)+k_z(rs)}\right] \quad (3)$$

$$\frac{\mathrm{d}Z(rs)}{\mathrm{d}t} = Z(rs)\left[\Gamma(rs)\,g(rs)\frac{F(s)}{F(s)+k_z(rs)} - \Delta\right] \quad (4)$$

$$F = \sum_{j=1}^{n} \alpha_j \beta \quad (5)$$

Eq. (2) is the equation for total nutrients N_T (µmol N l^{-1}), which is a sum of the dissolved nutrients N (µmol N l^{-1}), the phytoplankton biomass P (µmol N l^{-1}) in each of n size classes s (µm), and the zooplank-

ton biomass Z (µmol N l^{-1}) in each of the n zooplankton size classes. We note that size is a linear dimension, in this case equivalent spherical diameter (esd).

Eq. (3) describes the rate of change of the phytoplankton biomass of a given size class s. The first set of terms in this equation is a rectangular hyperbolic function that describes the growth of phytoplankton as a function of dissolved nutrient concentration, where is the maximum phytoplankton growth rate (d^{-1}) and k_s is the nutrient half-saturation constant for phytoplankton (µmol N l^{-1}). We assume that our growth component has metabolic losses (e.g. respiration, exudation) already incorporated into it. The middle term Λ is a general loss term (d^{-1}), which we consider to be non-grazing mortality. We consider it biomass-associated (e.g. autolysis, viral lysis, senescence, etc.) so as not to contain the metabolic processes already incorporated in the growth term. Sinking is not considered because the system is closed, with a constant sum of total nitrogen (Eq. 2). The third set of terms in Eq. (3) represents grazing mortality. Similar to phytoplankton growth, it also has a rectangular hyperbolic form in which g is the maximum zooplankton grazing rate (d^{-1}), k_z is the zooplankton grazing half-saturation constant (µmol N l^{-1}), and r is the predator-to-prey size ratio or the size ratio around which potential prey size classes are distributed. We recognize there are a variety of potential grazing functional forms (Gentleman et al. 2003). We followed the base model (Poulin & Franks 2010) and used a rectangular hyperbolic form. Its prevalence in the literature signifies its credibility as a grazing functional form and also facilitates our parameterization of the model. However, an interesting future study may include an examination of how changes in the grazing functional response influence the model dynamics (Franks et al. 1986, Gentleman & Neuheimer 2008).

Eq. (4) describes the rate of change of zooplankton biomass. The first set of terms describes zooplankton growth. It is similar to the final term in Eq. (3), since zooplankton grow from their consumption of phytoplankton. The dimensionless gross growth efficiency Γ is a measure of how much of the material ingested is converted into grazer biomass. Because Γ includes metabolism, it is different than the γ of the original Poulin & Franks (2010) model, which was assumed to be assimilation efficiency and thus did not include metabolic losses. This difference is reflected in the generic zooplankton loss term Δ (d^{-1}). In the original model, δ is the generic loss term and includes metabolism. Here, because that process is already accounted for in Γ, Δ is the loss rate due to biomass-associated processes, similar to Λ for phytoplankton.

F is the amount of food available to the grazers (µmol N l^{-1}). This term differentiates each model: it determines whether the zooplankton are herbivorous or omnivorous, how many size classes they consume, and how that consumption is distributed among prey size classes. The available food is modeled according to Eq. (5) where α, the grazing kernel, determines which phytoplankton and/or zooplankton size classes a zooplankter eats and how consumption is distributed among different size classes of prey items. In Model 1, zooplankton consume one phytoplankton size class based on the predator-prey size ratio r. In Models 2 and 3, zooplankton consume several prey size classes, denoted by η. In Model 2, zooplankton are herbivorous. They consume η consecutive phytoplankton size classes, the largest of which is determined by r. The proportion of grazing on each potential size class of phytoplankton is weighted by the abundance of prey in each of those size classes. In Model 3, zooplankton again consume η consecutive size classes, the largest of which is still determined by r. In this model the omnivorous predators consume η size classes of both phytoplankton and zooplankton, with the feeding preference weighted by the abundance of both prey types in the appropriate size classes. The variable β represents the prey types that a zooplankter can consume. For Models 1 and 2 in which the zooplankton are herbivorous, β = P. For Model 3, β includes both P and Z because the zooplankton predators are omnivores.

Model descriptions

Parameterization

To parameterize the models, we synthesized values from the literature. Each parameter value was converted to our units according to specific guidelines, which are described below. The sources and specific-values appear in the Supplement at www.int-res.com/articles/suppl/m514p013_supp.pdf. For all values for all parameters, if replicate experiments under identical conditions were performed in a single study, we used the average of those values. If a source included several experiments on the same organism under differing conditions, we used the value that most closely represented the parameter of interest (e.g. the experiment that produced the highest growth rate was used as the value for), and/or the experimental value that had the most information associated with it (e.g. the organism size, the temperature, etc.). After all the values for each parameter

were collected, the log-transformed values were regressed against log-transformed size values to find the coefficient and exponent (Eq. 1) and 95% confidence intervals for the size-dependent relationship for each parameter. For the zooplankton parameters (described below), we used values for protistan microzooplankton, not meso- or macrozooplankton. Therefore, the '*Z*' in the NPZ model specifically refers to non-metazoan grazers. From now on, we specifically refer to microzooplankton for our grazer community.

Cell size

We used equivalent spherical diameter (*esd*) as our metric of cell size. If a source provided cell volume v (μm^3), *esd* was calculated using the equation $esd = (6v/\pi)^{1/3}$. If linear dimensions (i.e. length and width) values were listed, those values were first converted to a volume assuming the cell was a prolate spheroid, according to the equation $v = lw^2\pi/6$, where l is the length (µm) and w is the width (µm). After that, the previous equation was used to calculate *esd*. If no measure of cell size was indicated in the original study, additional relevant literature sources for the species were used for size information.

Maximum phytoplankton growth rate

Maximum phytoplankton growth rate values (□) were all converted to maximum specific growth rates (d^{-1}). If the value was given in doublings per day, it was converted to specific growth rate according to the equation □ = (divisions d^{-1})/ln(2). We corrected the rates to 20°C using the metabolic theory of ecology approach (Brown et al. 2004), in which a metabolic rate R is assumed to vary with temperature T (in K), mass size dependence M^A, and activation energy E according to the equation $R = R_0 e^{-E/kT} M^A$ where R_0 is a constant and k is Boltzmann's constant (-8.62×10^5 eV K^{-1}). Specifically, we used the concepts outlined in Chen et al. (2012) to correct all values to a single temperature, using their estimate of growth activation energy of 0.36 eV. Specific growth rate values and sources are given in Table S1 in the Supplement.

Using this methodology, maximum phytoplankton growth rate was found to decrease with increasing size (Fig. 3a, Table 1): larger phytoplankton had a lower maximum specific growth rate than smaller phytoplankton. This relationship is based on 101 temperature-corrected data points, with $r^2 = 0.12$. Although this coefficient of determination is low, that is, limited variability is explained by size, the relationship was still significant ($p < 0.05$). We discuss potential reasons in the 'Results and discussion'. The temperature-corrected rates were compared with the uncorrected rates to calculate traditional Q_{10} values according to the equation

$$\left(\frac{\omega_{20}}{\omega}\right)^{\frac{10}{20-T}} = Q_{10}$$

where ω_{20} is the temperature-corrected value, ω the uncorrected value, and T is the experimental temperature (in °C). These Q_{10} values ranged from 1.60 to 1.64, which, while slightly smaller than the commonly used value of 1.88 of Eppley (1972), are still not unreasonable.

Phytoplankton half-saturation constant

Phytoplankton half-saturation constant (k_s) values were taken from various sources (Table S2). No distinction was made between the uptake of nitrogen in different forms (e.g. ammonium, nitrate). If uptake of one or more forms of nitrogen were recorded in a single source for the same organism but in separate experiments (e.g. ammonium uptake was measured in one experiment and nitrate in another), the values

Table 1. List of parameters estimated from a compilation of literature sources. NA = not applicable

Parameter	Coefficient (95% CI)	Exponent (95% CI)	Units
Total nutrients, N_T	15 (NA)	NA	µmol N l^{-1}
Grazing half-saturation constant, k_z	17.92 (7.64, 42.05)	−0.64 (−0.92, −0.35)	µmol N l^{-1}
Maximum grazing rate, g	33.96 (15.02, 76.80)	−0.66 (−0.94, −0.37)	d^{-1}
Gross growth efficiency, Γ	0.31 (0.13, 0.79)	−0.02 (−0.32, 0.28)	dimensionless
Microzooplankton loss rate, Δ	0.025 (NA)	0 (NA)	d^{-1}
Phytoplankton half-saturation constant, k_s	0.33 (0.16, 0.68)	0.48 (0.23, 0.73)	µmol N l^{-1}
Maximum phytoplankton growth rate, □	1.36 (1.04, 1.78)	−0.16 (−0.25, −0.07)	d^{-1}
Phytoplankton loss rate, Λ	0.0015 (NA)	0 (NA)	d^{-1}

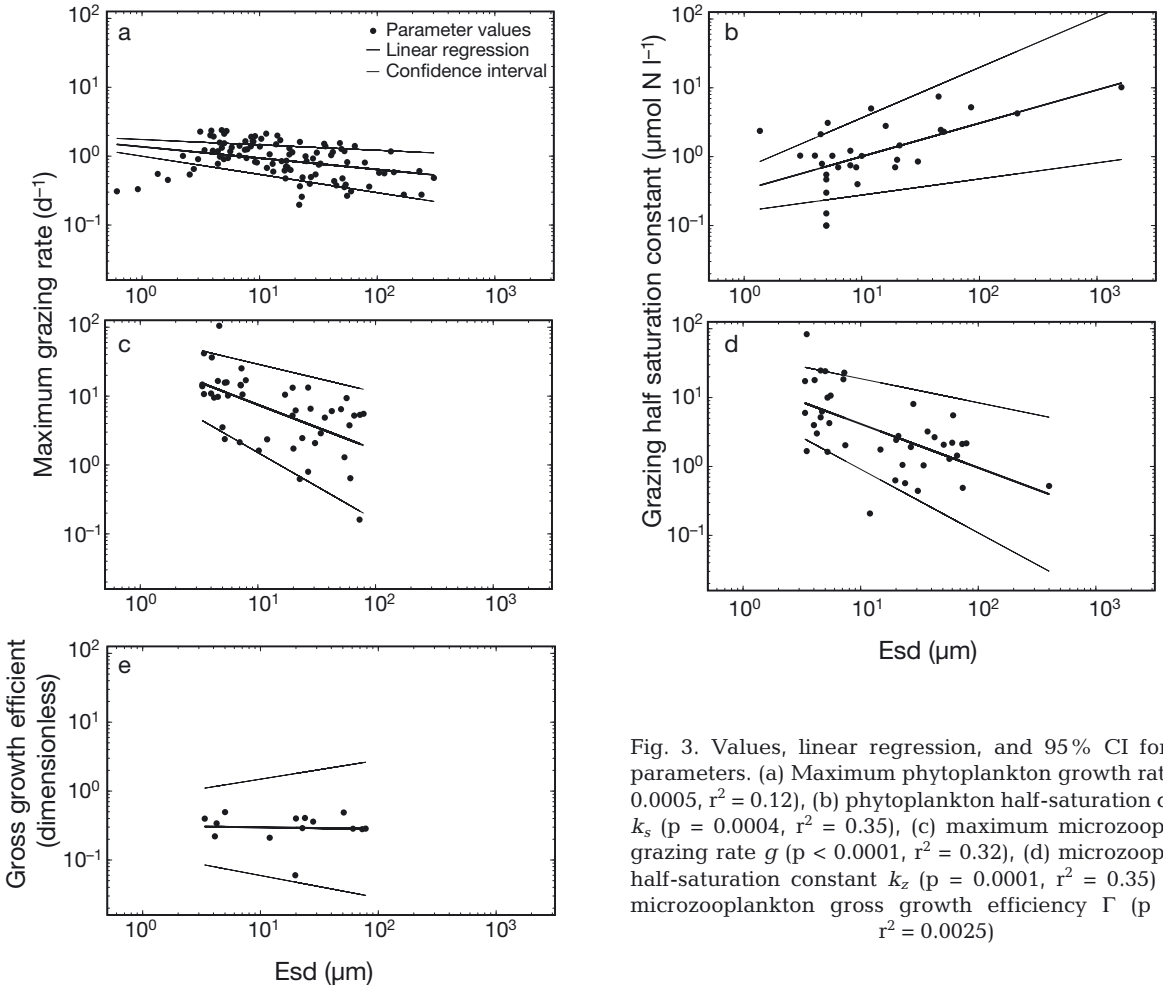

Fig. 3. Values, linear regression, and 95% CI for model parameters. (a) Maximum phytoplankton growth rate □ ($p = 0.0005$, $r^2 = 0.12$), (b) phytoplankton half-saturation constant k_s ($p = 0.0004$, $r^2 = 0.35$), (c) maximum microzooplankton grazing rate g ($p < 0.0001$, $r^2 = 0.32$), (d) microzooplankton half-saturation constant k_z ($p = 0.0001$, $r^2 = 0.35$) and (e) microzooplankton gross growth efficiency Γ ($p = 0.87$, $r^2 = 0.0025$)

were averaged. Where possible, size values were taken from the original source, and additional sources were used otherwise. With our compilation, the phytoplankton half-saturation constant showed an increase with increasing size (Fig. 3b, Table 1; 31 data points, $r^2 = 0.45$, $p < 0.001$). Thus, larger phytoplankton require a higher nutrient concentration to reach half their maximum growth rate compared to smaller cells.

Phytoplankton loss rate

We assumed that phytoplankton loss rate (Λ) includes what we term 'biomass-associated losses', such as viral loss and autolysis. That is, the loss rate is a constant fraction of the biomass. Little information is available about non-grazing mortality of phytoplankton (see Bidle & Falkowski 2004 for a review). One of the best-studied forms of loss is viral lysis (Brussaard 2004). However, most literature values of viral loss are associated with bloom conditions (e.g. van Boekel et al. 1992, Brussaard et al. 1995, 1996). Little is known about the rates of viral loss in normal conditions for specific organisms (although see, for example, Suttle & Chan 1994 and Cottrell & Suttle 1995). Furthermore, Λ encapsulates all forms of biomass-associated loss. While the dissolved esterase method (van Boekel et al. 1992, Agusti et al. 1998, Riegman et al. 2002) is a measure of total cell lysis, from viruses or otherwise, the method has been described as semi-quantitative (van Boekel et al. 1992, Riegman et al. 2002). Therefore, we have somewhat arbitrarily chosen a value for non-grazing associated loss to be 0.0015 d^{-1}. This value was chosen based on its ability to produce reasonable size spectra (i.e. slope and intercept values), a realistic phytoplankton: microzooplankton biomass ratio, and a reasonable size range. While this value may seem low, it is at least within an order of magnitude of the total cell lysis rates measured by Riegman et al. (2002) using the dissolved esterase method, which, although semi-

quantitative, makes an attempt to measure all loss sources considered in this parameter. Furthermore, because so little is known about this loss rate, a small value for Λ may indeed be appropriate. Also due to the lack of knowledge regarding loss rate values, we used a constant value for all size classes (i.e. no scaling exponent). We are aware that this parameter may be size-dependent (Weinbauer & Hofle 1998, Brown et al. 2004; see 'Results and discussion' for details) and hope that future studies will help determine its value specifically for phytoplankton.

Maximum microzooplankton grazing rate

For maximum microzooplankton grazing rate (g), values were mainly taken from Hansen et al. (1997), complemented by more recent studies. A complete list of sources is given in Table S3. For sources listed in Hansen et al. (1997), cell-size values were taken from that source. Volume was converted according to the description above. However, Hansen et al. (1997) provide specific grazing rates that are normalized by biovolume. Here, we normalized by nitrogen content of the prey and grazer. If nitrogen values were not listed in the original source, they were taken from other studies. Also, for all values, if only carbon was given or calculated, we converted to nitrogen using the Redfield ratio (106 C:16 N).

When converting from grazer biovolume to nitrogen content, we used published relationships for the specific grazer type. For nanoflagellates, we used the relationship from Borsheim & Bratbak (1987), and for dinoflagellates and ciliates, we used relationships from Menden-Deuer & Lessard (2000). Because the prey items were more diverse, we converted from biovolume to nitrogen content using sources specific to the prey organism.

Similar to □, we corrected grazing rate values to 20°C using the work of Chen et al. (2012) and their estimate of grazing-associated activation energy of 0.67 eV. Using this correction, g varied inversely with size (Fig. 3c, Table 1) and was significant ($r^2 = 0.32$, $p < 0.01$, $n = 46$). This relationship is based on the temperature-corrected values. Similar to what was described above for □, we compared these g values with the uncorrected rates to compute the Q_{10} values to which our corrections correspond. These corresponding Q_{10} numbers varied from 2.43 to 2.53, which are within the range of values estimated for a variety of microzooplankton (e.g. Aelion & Chisholm 1985, Verity 1985, Caron et al. 1986, Choi & Peters 1992).

Grazing half-saturation constant

To convert grazing half-saturation constant values (k_z) from units used in the literature to µmol N l^{-1}, we used conversion values of the prey items (e.g. cell size, cell nitrogen content), when possible, from the source for which the half-saturation constant was taken. If those values were not available, we used values from other sources. A complete list of sources and values is given in Table S4. Using those values, grazing half-saturation constant (Fig. 3d) was found to vary inversely with size ($r^2 = 0.35$, $p < 0.01$, $n = 40$; Table 1).

Gross growth efficiency

To parameterize the gross growth efficiency (Γ), we used several sources listed in Table S5. Values were either taken directly from the study or calculated according to the equation Γ = growth rate/grazing rate. When there was more than one potential value (e.g. more than one experiment was conducted in a study), we used the value that corresponded to the maximum grazing rate and the growth rate most closely associated with the maximum grazing rate conditions. All values are dimensionless.

Plotting gross growth efficiency Γ against size (Fig. 3e), we found no dependence on size ($r^2 = 0.003$, $p = 0.84$, $n = 14$; Table 1), with the confidence intervals encompassing zero. Therefore, in our analyses below, we used the average value of 0.32 (Table 1).

Microzooplankton loss rate

Similar to the phytoplankton loss rate (Λ), we assumed the microzooplankton loss (Δ) is biomass-associated. Furthermore, just as with phytoplankton, little is known about non-grazing mortality of microzooplankton. Nagasaki et al. (1993) found viruses to infect ~20 % of a population of an unknown flagellate associated with a bloom of *Prorocentrum triestinum*. Garza & Suttle (1995) were the first to isolate a naturally occurring virus that affects a marine heterotroph, *Cafeteria roenbergensis* (originally misidentified as *Bodo* sp.), in waters off Texas. However, only recently has this virus been studied genetically in detail (Fischer et al. 2010). A population of *C. roenbergensis* declined in incubation experiments in the Indian Ocean, presumably due to viral lysis (Massana et al. 2007), and Saura et al. (2011) found viruses to negatively affect populations of heterotrophic flag-

ellates, either directly through lysis or indirectly through bacterial lysis.

While these studies highlight that non-grazing mortality, particularly due to viruses, may be important in regulating microzooplankton populations, the relatively sparse information on this topic limits our parameterization of this variable. Therefore, we selected the value of 0.025 d^{-1} for microzooplankton loss which helps fulfill our criteria, mentioned above, of producing a realistic phytoplankton:microzooplankton biomass ratio and planktonic size range. Also because of the lack of information, we chose not to make this variable size-dependent (i.e. the scaling exponent is zero), but see the 'Results and discussion' for a more detailed description.

Other parameters

The modeled size classes range from ca. 0.8 µm to 65 mm, determined from the equation $0.8 \times (1.0182^{j})$, where j ranges from 0 to 500. For simplicity, and because microzooplankton often consume prey of similar size to themselves, we chose a constant predator-prey size ratio r of 1. While variation in this parameter has the potential to lead to interesting dynamics, we chose to focus on the variable trophic dynamics among each model rather than within each model. Also, the number of size classes grazed upon in Models 2 and 3 was set to 5. Therefore, size class j can graze upon organisms between $0.8 \times (1.02^{j-2})$ to $0.8(1.02^{j+2})$ µm. To examine how the phytoplankton and microzooplankton size spectra change under differing nutrient regimes, we varied the total nitrogen in the system N_T among the values 10, 20, 25, and 30 µM N in each of the 3 models.

RESULTS AND DISCUSSION

Parameterization

In our synthesis of updated literature values to describe the size dependency of planktonic variables, we have compromised between specificity and generality. For example, we chose to focus explicitly and in detail on protistan microzooplankton, to the exclusion of larger metazooplankton. Because microzooplankton are often the main grazers in a community (Calbet & Landry 2004), this focus allowed us to more realistically simulate the impact and dynamics of these important planktonic components.

We also generalized our parameterizations by combining different functional groups of both phytoplankton and microzooplankton. While other studies have argued for distinguishing among various taxa or groups (e.g. Banse 1982, Edwards et al. 2012), as discussed in more detail below, our combination of various organisms makes the parameterizations, and subsequently the model, more generalizable and thus more applicable to a wider variety of ecosystems. These syntheses of planktonic rates will help increase our understanding of a fundamental property — size-dependence — which underlies important planktonic dynamics observed in nature. These allometric relationships also aid in modeling natural communities by simplifying the rate parameterizations for diverse components of planktonic assemblages.

We also put these size-dependent patterns in the context of previously published allometric scalings. Because our motivation was to determine the allometric scaling of variables in the Poulin & Franks (2010) model and our units (*esd*, d^{-1}, µmol N l^{-1}, etc.) may differ from choices in other parameterizations, comparisons between this and other studies are qualitative at best. Within our modeling context, we were also able to examine how these underlying processes shape the planktonic community under various nutrient regimes.

Phytoplankton parameterization

The debate about the relationship of phytoplankton growth rate with size is highlighted in early studies on the subject. Williams (1964) and Eppley & Sloan (1966) both found negative correlations between size and growth rate for phytoplankton. Fenchel (1974) extended the relationship between maximum growth rate and weight to a variety of organisms. Different groups of organisms had different relationships, but all decreased with size. Banse (1976) also found a decrease in size among single-celled autotrophs. However, a revision of his work and those of others (Banse 1982) led to a weaker relationship, which was different for diatoms compared to dinoflagellates. Similarly, Chan (1978) and Sommer (1989) found a weak relationship of growth rate with size for marine autotrophs. However, Mizuno (1991) examined the size-dependence of growth rate for 19 species of aquatic diatoms and also reviewed these early studies. He found that growth rate did indeed decrease with size, that the relationship was significant, and that the relationship he found was not significantly different from most of the previously published studies. Tang

(1995) did a more extensive study of the size-dependence of algal growth rates and also found a significant decrease with size that was not markedly different from these previous works.

More recently, Edwards et al. (2012) found a decrease in maximum autotrophic growth rate with increasing size for both marine and freshwater species. Furthermore, the relationship was different between the 2 groups. In this study, however, we have included only marine and estuarine species and thus have not made any distinction between them. Taken together, these studies give us confidence that the size dependencies in relation to growth are real.

However, adding to the debate about the size-dependence of □, there is now evidence to suggest that the relationship may be more complex. While larger organisms may show a decreasing trend in maximum growth rate with increasing size, recent studies have demonstrated that smaller phytoplankton may show the opposite trend (Bec et al. 2008, DeLong et al. 2010, Kempes et al. 2012, Marañón et al. 2013). That is, there is a unimodal relationship between phytoplankton size and growth rate. Indeed, with the inclusion of data from Marañón et al. (2013) in our synthesis, we see a number of lower values at the small end of our size range (Fig. 3a).

Nevertheless, even with these data, we still found a significant decrease in □ with size ($p < 0.05$). Therefore, while we acknowledge that there may be more fine-scale structure within the parameterization of □, for simplicity and to continue our compromise between generality and specificity, we still used a monotonic trend in maximum growth rate with size. However, we do note that the size dependencies measured in this study may not hold in the field. For example, variable taxonomic composition, resource limitation, and the interaction of trophic levels may lead to different size dependencies than those estimated here (Marañón et al. 2007, Chang et al. 2013).

Contrary to the phytoplankton growth rate, the phytoplankton half-saturation constant showed a monotonic increase with increasing size. Thus, relatively larger phytoplankton need a higher nutrient concentration to reach half their maximum growth rate compared to smaller phytoplankton. The increase in half-saturation constant with size has also been shown before. Eppley et al. (1969) found that larger cells have higher half-saturation constants than smaller cells. Furthermore, they found that faster-growing cells have lower half-saturation constants than slower-growing cells, which is also supported by the allometric relationships in this study. When specifically examining the allometric relationship, Litchman et al. (2007) found a positive scaling between cell volume and half-saturation constant—at least when comparing across, rather than within, taxonomic groups. Edwards et al. (2012) also found an increase in nitrogen half-saturation constant with increasing cell volume. Similar to maximum growth rate, they found a significant difference between the relationships for freshwater species and marine organisms. Our parameterization only included marine species and so does not warrant this comparison.

Concerning the phytoplankton loss rate, the Metabolic Theory of Ecology (MTE; Brown et al. 2004) suggests that all mortality sources combined should scale with mass with a −0.25 scaling exponent. We could have used this idealized relationship as justification for a size-dependent loss rate Λ. However, we were hesitant to use such a parameterization for several reasons. MTE is an equilibrium theory, based on the assumption that net population growth is zero. Thus, because fecundity rates have a −0.25 size-dependent scaling exponent, so should mortality. However, we did not want to assume equilibrium *a priori* in our parameterization. Our parameter values were also based specifically on empirical planktonic data, avoiding organisms other than those specifically modeled. While MTE proposes scaling relationships that hold for all types of life, the empirical information supporting the mortality rates are based on fish (Brown et al. 2004). Furthermore, there is evidence that r^2 values for the allometric relationships based on MTE decrease with decreasing size range (Tilman et al. 2004). Therefore, the large size range seen in the fish-based relationship may not hold equally well among phytoplankton. Thus, we refrained from using the MTE scalings and instead used the size-independent mortality rate. However, we note that the effect of a size-dependent Λ on the spectral slope can be calculated by rearranging terms in the model equations (see the subsection 'Planktonic spectral slopes' for a detailed description of this method).

Because larger phytoplankton have a lower maximum growth rate, require higher nutrient concentrations to reach half their maximum rate, and loss is modeled as constant for all size classes, smaller phytoplankton are at an advantage in the absence of predation. That is, relatively smaller phytoplankton would be competitively dominant without grazers. However, this comparison of maximum growth rate and half-saturation constant, while important within our model construct, may not be the best metric of competitive ability. A better measure of a cell's competitive ability is given by the nutrient affinity (But-

ton 1978, Healey 1980). Having a high affinity means an organism is more competitive at taking up resources (Healey 1980). The half-saturation constant can be derived from the ratio of the maximum nutrient uptake rate and the nutrient affinity.

Because we do not have measurements of the maximum uptake rate, we did not calculate the nutrient affinity. However, Litchman et al. (2007) did examine the relationship between several parameters, including maximum nutrient uptake rate, half-saturation constant, and maximum growth rate. Similar to our study, they found that maximum phytoplankton growth rate correlated negatively with the half-saturation constant. Because a high maximum uptake rate and low half-saturation constant would both lead to competitive superiority, those 2 values do not constitute a tradeoff.

Microzooplankton parameters

Our observed decrease in maximum grazing rate with increasing size (Fig. 3c) is supported by previous studies. Given that much of the data used in this study came from Hansen et al. (1997), it is not surprising that they had a similar negative relationship between predator volume and maximum ingestion rate, both when examining their entire data set and within specific subgroups (e.g. metazooplankton, dinoflagellates, etc). Fenchel (1980) found a similar inverse relationship, based on compiled measurements of ciliates, and Moloney & Field (1989) also used a negative exponent in their allometric relationships between maximum specific ingestion rate and body mass. Contrary to these results, Peters (1994) found that ingestion rate increased with increasing predator volume. However, for his study, realized ingestion rate rather than maximum ingestion rate was used.

Similar to g, the grazing half-saturation constant k_z (Fig. 3d) decreased with increasing size. However, unlike g, support from the literature for this parameter is not as clear-cut. For instance, Hansen et al. (1997) did not find a significant relationship between size and grazing half-saturation constant. However, this result may be partly due to the method of calculation. k_z was determined from the ratio of maximum clearance rate and maximum ingestion rate. Because a common slope was forced through both, k_z was independent of size. However, they did find a significant relationship when examining subsets of their data. Specifically, the protozooplankton had a significant negative relationship between k_z and cell volume, while the dinoflagellates had a positive relationship. Nevertheless, they do point out that ciliates, which were generally larger in size, had lower k_z values than did dinoflagellates, which were generally smaller.

Fenchel (1980) examined the grazing half-saturation constant for several ciliate species but did not compare it directly with size. Instead, he looked at its relationship with optimal prey size and found an inverse relationship. In this study, grazer size was proportional to prey size with a 1:1 ratio. Therefore, assuming these are their optimal prey sizes (these are the only particles they can eat), an inverse relationship between k_z and optimal prey size is equivalent to an inverse relationship between k_z and grazer size.

Contrary to the above microzooplankton parameters, gross growth efficiency Γ (Fig. 3e) was size-independent. Straile (1997) found gross growth efficiency to be independent of grazer functional group, with mean and median values between 0.2 and 0.3. Hansen et al. (1997) also found no difference among taxonomic groups, with a mean value of 0.33. While neither study specifically examined the size-dependency of this parameter, the lack of differentiation among various types of grazers, which can be considered to roughly correspond with changes in size, helps support the size-independence of Γ.

For the microzooplankton, the maximum ingestion rate may be considered similar to the maximum nutrient uptake rate for phytoplankton, given that they are both a direct measure of uptake of resources. Similar to the tradeoff between maximum nutrient uptake and half-saturation constant seen for phytoplankton (Litchman et al. 2007), we saw a tradeoff in k_z and g for microzooplankton. That is, the size-dependent relationship of g indicates that larger microzooplankton graze at a lower maximum rate than do smaller grazers. However, they also have a lower half-saturation constant compared to smaller grazers. Therefore, at lower prey concentrations, larger microzooplankton have higher grazing rates than smaller microzooplankton. However, due to the competitive advantage of smaller phytoplankton, there are smaller abundances of prey items for larger microzooplankton. At higher prey concentrations, smaller microzooplankton have a higher specific grazing rate.

For the microzooplankton loss term Δ, we could have used MTE to guide our parameterization. However, the same general arguments for the phytoplankton loss term (see subsection 'Phytoplankton parameterization') also apply to Δ. That is, given the equilibrium assumptions of MTE and the lack of mor-

tality estimates specifically for microzooplankton, we chose to use a size-independent Δ.

Modeled size distributions

Using the estimated parameter values described above, we created steady-state size spectra from each of the 3 size-structured NPZ models. Model 1, with herbivorous grazing on one size class of phytoplankton (Fig. 2a), has an analytical steady state solution (Poulin & Franks 2010). That solution was used to calculate the phytoplankton and microzooplankton size spectra at each of the 4 total nutrient concentrations (Figs. 4 & 5). The spectra from Models 2 and 3 were quite similar to those of Model 1, which we describe in detail.

With increasing N_T, the phytoplankton size range elongates, meaning that biomass is added to larger size classes. For example, at 10 µM N, phytoplankton ranged in size from ca. 0.81 µm to 39 µm (Fig. 4a), while at 30 µM N the largest size class was 1915 µm (Fig. 4d). However, the slope and intercept changed very little, maintaining values around −0.95 µM N μm^{-2} and 2.20 µM N μm^{-1}, respectively, for all nutrient concentrations (Table 2). Therefore, for Model 1, increased total nutrient concentration did not affect the phytoplankton biomass in existing size classes but rather expanded the size range to include increasingly larger sized cells.

For the Model 1 microzooplankton size spectra, both the biomass in existing size classes and the size range increased at higher nutrient concentrations (Fig. 5). For example, the biomass of 1 µm cells increased from 0.44 µM N μm^{-1} at N_T 10 µM N to 5.26 µM N μm^{-1} at N_T 30 µM N (Table 2). Furthermore, the largest size class increased from ~40 µm at 10 µM N_T (Fig. 5a) to ~1880 µm at 30 µM N_T (Fig. 5d). While the spectra dropped off drastically at larger size classes, regressions of the linear portion of each microzooplankton spectrum revealed that the spectra are steeper than for phytoplankton, with values around −1.7 µM N μm^{-2} that slightly decrease in magnitude with increasing nutrient concentrations (Table 2). That is, for a given nutrient concentration, microzooplankton biomass decreased more rapidly with size than did phytoplankton biomass, but the decrease became slightly less drastic as total nutrients increased.

Model 2, which includes herbivorous grazing on multiple phytoplankton size classes (Fig. 2b), and Model 3, which allows omnivorous predation on multiple size classes of phytoplankton and microzooplankton (Fig. 2c), do not have steady-state solutions. To estimate steady-state biomasses at a given N_T, we initialized both models with the Model 1 steady-state solution at that N_T value. We then ran each model forward in time for 30 yr and averaged the biomass value in each size class for the last 10 yr. These decadal averages were used as our estimates of steady-state spectra for Models 2 and 3 for each total nutrient concentration (Figs. 4 & 5).

On different time scales and/or under variable conditions, different dynamics may be observed. For example, on shorter time scales, there may be large variability within and among size classes, perhaps due to predator-prey oscillations. There is also evidence from the field that during a bloom situation, some organisms may increase disproportionately to others, forming a domed size spectrum among the larger size classes (Zarauz et al. 2009). However, while there may be interesting transient dynamics on shorter timescales, we have chosen to examine these long-term averages to better focus on the fundamental dynamics and basic model behavior among these 3 models under different nutrient regimes.

While these biomass spectra were not as smooth as for Model 1, the greater variability is not surprising given the increased food web complexity of Models 2 and 3. Furthermore, both models still produced normalized size spectra that decrease with increasing size, a common feature of planktonic size spectra (Rodriguez & Mullin 1986, Sprules & Munawar 1986).

Model 2 produced microzooplankton and phytoplankton spectra remarkably similar to Model 1. The

Table 2. Regression parameters from fit to linear portion of size-specific planktonic biomass spectra under different total nutrient concentrations for Models 1, 2, and 3

Model Regression parameter	10 µM N	20 µM N	25 µM N	30 µM N
1				
Phytoplankton slope	−0.98	−0.96	−0.95	−0.95
Phytoplankton intercept	2.28	2.23	2.19	2.14
Microzooplankton slope	−1.82	−1.69	−1.67	−1.65
Microzooplankton intercept	0.44	2.31	3.75	5.26
2				
Phytoplankton slope	−0.98	−0.97	−0.97	−0.97
Phytoplankton intercept	2.27	2.25	2.24	2.24
Microzooplankton slope	−1.85	−1.71	−1.65	−1.63
Microzooplankton intercept	0.49	2.45	3.73	5.20
3				
Phytoplankton slope	−1.04	−1.12	−1.15	−1.17
Phytoplankton intercept	2.66	3.95	4.72	5.50
Microzooplankton slope	−1.90	−1.81	−1.79	−1.78
Microzooplankton intercept	0.44	1.99	2.29	4.08

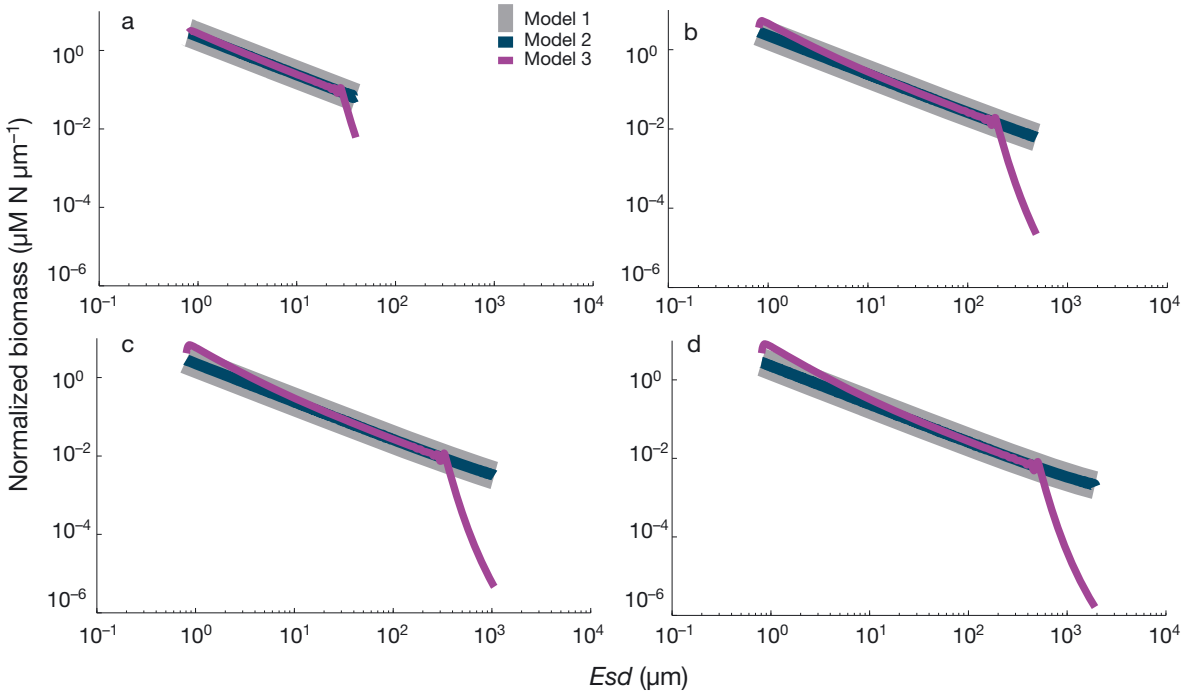

Fig. 4. Normalized steady state phytoplankton for Models 1, 2, and 3, at total nutrient concentrations of (a) 10 µM N, (b) 20 µM N, (c) 25 µM N and (d) 30 µM N

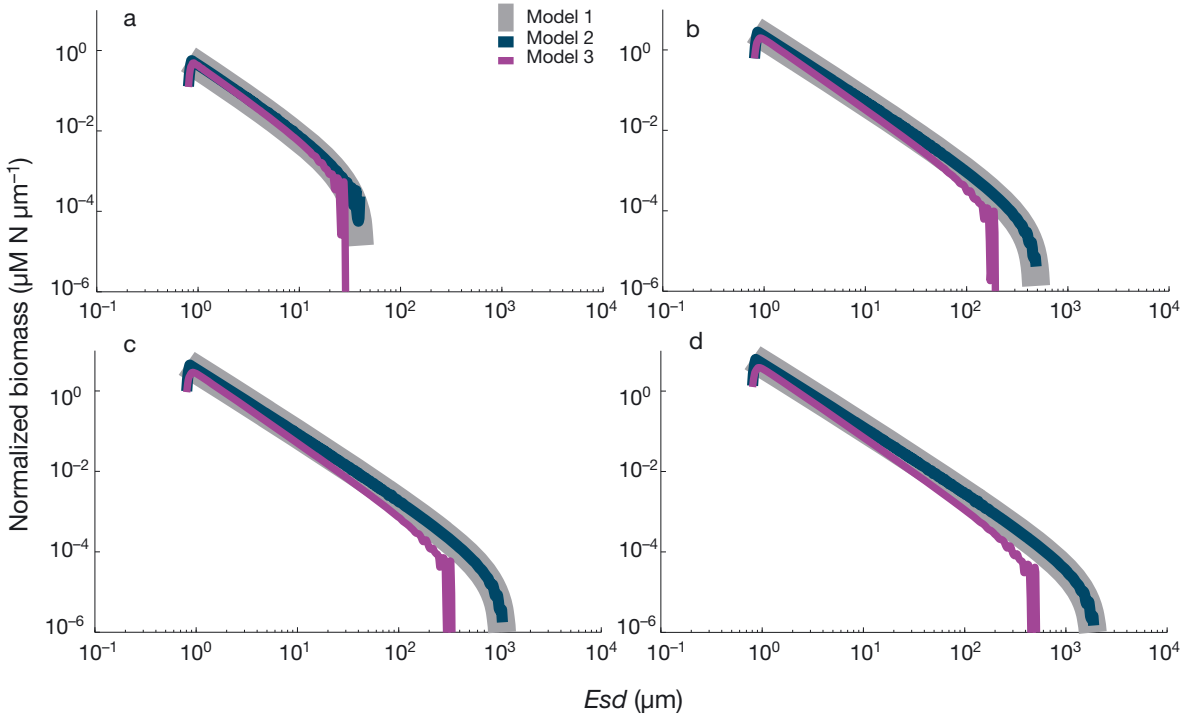

Fig. 5. Normalized steady state microzooplankton for Models 1, 2, and 3, at total nutrient concentrations of (a) 10 µM N, (b) 20 µM N, (c) 25 µM N and (d) 30 µM N

phytoplankton size range elongated with increasing nutrient concentration (Fig. 4). The intercept and slope values were also very close to those of Model 1 (Table 2). Similarly, the microzooplankton spectra increased in size range at higher nutrient concentrations (Fig. 5) and also had linear fits close to those of Model 1 (Table 2). Distinct from Model 1, the Model 2 microzooplankton spectra had a decrease in biomass at the smallest size range (Fig. 5).

The inclusion of omnivory in Model 3 produced slightly different spectral patterns from the other models. Though the spectra are less smooth, the general decrease in normalized biomass with increasing size was still preserved, despite the more complex feeding connectivity (Figs. 4 & 5). There was also a steep drop in biomass of the largest size classes for both phytoplankton and microzooplankton. For a given nutrient concentration, this decrease in biomass occurred at approximately the same size in both plankton types, indicating a close coupling of microzooplankton and phytoplankton.

In addition to the sharp decrease in biomass among the largest cells, the phytoplankton spectra had steeper slopes and higher intercepts than those of the other 2 models at a given total nutrient concentration (Table 2). Therefore, smaller phytoplankton were more numerous and proportionately more abundant than large cells in Model 3 compared to the other models. Also unique to this model, these characteristics were exaggerated as nutrient concentration increases (Fig. 4, Table 2). However, similar to the other models, there was an elongation of the size spectra with increasing N_T.

The microzooplankton spectra in Model 3 are also similar to the other models in that the slopes become shallower, the intercepts higher, and the largest size class greater with increased total nutrient concentration (Fig. 5, Table 2). However, the microzooplankton spectra have steeper slopes and lower intercepts than the models with only herbivory. Taken together, all 3 models represent an improvement over the original model (Poulin & Franks 2010) because they allow the direct comparison of the effects of trophic strategy on the planktonic communities.

Overall, for all nutrient concentrations considered, there was a decrease in the relative proportion of normalized phytoplankton and microzooplankton biomass with increasing size regardless of the specificity of the microzooplankton feeding (single-prey herbivorous, multiple-prey herbivorous, multiple-prey omnivorous; Figs. 4 & 5). Therefore, this structuring of planktonic communities is a robust feature of our modeled ecosystems, regardless of trophic dynamics. Such negative slopes for both planktonic spectra have been observed in aquatic systems. For example, Rodriguez & Mullin (1986) found a decrease in normalized biomass of both 'microplankton' and 'macroplankton' in the north Pacific gyre (Fig. 1). In freshwater systems, Ahrens & Peters (1991) and Sprules & Munawar (1986) also found downward-sloping normalized biomass spectra of plankton in various North American lakes. We do note that the sharp decrease in biomass seen in our model spectra among large size classes, particularly among the microzooplankton, is not typically seen in spectra from field samples. While such results may be due to limitations in our model, the discrepancies may also result from differences in the size resolution.

As nutrients and/or total biomass increase, there is often an increase in the relative proportion of large plankton compared to small plankton (Sprules & Munawar 1986, Ahrens & Peters 1991, Chisholm 1992, Landry 2002, Uitz et al. 2006, Ward et al. 2012, Ho et al. 2013). Such an increase in the relative importance of larger plankton can occur in 2 non-mutually exclusive ways: (1) by changing the spectral slope b to give a shallower spectrum, or (2) by an extension of the size spectrum toward larger sizes with no change in the spectral slope. While there is evidence to support both possibilities (Chisholm 1992, Cavender-Bares et al. 2001, Zarauz et al. 2009), all our models support the second hypothesis: there was a consistent elongation of the phytoplankton and microzooplankton size range with increasing nutrient concentration (Figs. 4 & 5). In agreement with observations, this indicates an increase in the relative proportion of the large size classes and an overall increase in the total biomass of both state variables with increasing total nutrients/biomass (Ahrens & Peters 1991, Chisholm 1992). These characteristics occurred in all models through an elongation of the size range with increasing nutrients; only the model with omnivory showed an additional small steepening of the phytoplankton spectrum with increasing total nutrient (Fig. 4, Table 2). This steepening tended to decrease the relative proportion of large cells.

The elongation of the size range in all models is consistent with other models (Armstrong 1994, Thingstad 1998, Irwin et al. 2006, Ward et al. 2012) and with field data (Raimbault et al. 1988, Zarauz et al. 2009). Raimbault et al. (1988) and Chisholm (1992) suggest that as total biomass increases, a given size class of phytoplankton may reach a biomass threshold; total biomass is only increased by adding larger

phytoplankton size classes. However, we do note that this feature may only hold in nature for the largest and smallest plankton (Goericke 2011). While the microzooplankton in all our models tended not to behave this way (the biomass of each size class increased with total biomass), the phytoplankton size classes did. Thus, as nutrient concentration increased, larger phytoplankton size classes were created while the biomass in the smaller size classes remained saturated.

Overall, our model results show similarities with size distributions seen in the field. Zarauz et al. (2009) examined changes in the planktonic community throughout a bloom event: the spectra of the largest size classes changed shape during bloom, including via the addition of larger size classes—similar to the results in our study. Sprules & Munawar (1986) also generally observed shallower slopes with increased eutrophy. However, their size spectra were a combination of phyto- and zooplankton. They note that, with increasing eutrophy, phytoplankton abundances change little while those of zooplankton increase. We see related results in that, with increased nutrients, all of the microzooplankton size classes increased in biomass (i.e. there is an increase in intercept and a negligible change in slope), while the existing phytoplankton size classes did not change (little variation in slope and intercept). Therefore, phytoplankton biomass supports increased microzooplankton biomass with increasing eutrophy both in our models and in the field. San Martin et al. (2006) did not find a significant pattern between slopes and productivity (which they examined as nutrients, biomass, and primary production), just as we did not see significant changes in slope with nutrients. In contrast, there is also evidence that spectral slopes flatten with increased nutrients. For example, Cavender-Bares et al. (2001) found planktonic biomass of larger cells to increase in nutrient addition experiments in the Sargasso Sea (although not in the equatorial Pacific). While not consistent among all their study regions, they also found positive relationships between spectral slope and ambient nutrient concentrations in the Sargasso Sea and the northern region of the Gulf Stream.

Our model results can be compared with those from other size-structured models to assess their strengths and limitations and to highlight the similarities and differences in model structure and dynamics. Stock et al. (2008) modeled the steady-state structure of several trophic levels, from picoplankton to fish. With the inclusion of these higher predators, the effect of trophic cascades on different size classes can be observed. This was a limitation in our own size-structured models, but has the potential to be added in future studies.

Stock et al. (2008) also observed total biomass to increase and spectral slope to be constant with increasing nutrient flux, similar to this study. However, instead of an elongation of the size distribution, total biomass was increased by its addition to each size class. Such differences could be partially due to differences in size resolution and spectra composition: they considered only 3 size classes of phytoplankton and 4 of zooplankton while we considered hundreds, and their size spectra were a mixture of both phytoplankton and zooplankton. If we were to combine our phytoplankton and zooplankton size spectra, we would also see an increase in biomass of all size classes, in addition to the elongation of the size distribution, due to the increase in biomass of all size classes of microzooplankton with nutrient addition.

In another study, Fuchs & Franks (2010) created a highly resolved size-based omnivorous model with a structure similar to the ones here, particularly Model 3. However, there are some important differences. For example, they only examine one type of model, an omnivorous model, while here our juxtaposition of 3 different models allows us explicitly to examine the effects of differing trophic dynamics. Fuchs & Franks (2010) also use a different parameterization for their model and include only 2 size-specific terms: phytoplankton maximum growth rate and the zooplankton feeding kernel. This study more thoroughly addresses size-specificity by including more allometric relationships, supported by parameterizations specifically for plankton. The grazing kernel in Fuchs & Franks (2010) was modeled as a Laplace distribution, centered on the preferred prey size class. We did not use that particular functional form here, given the lack of concrete support for that specific form (Fuchs & Franks 2010). Also in the Fuchs & Franks (2010) model, organisms at the extremes of the size range consume less because they have a truncated prey size range, and the prey size classes that remain do not compensate for the decreased consumption. This is different from our model formulation, in which grazers consume the maximum prey possible from other size classes when size classes at the ends are not available.

Similar to our results, the model from Fuchs & Franks (2010) generally increased the number of size classes with increasing nutrients. For phytoplankton, however, they also observed a decrease in the number of size classes with eutrophication, particularly for lower predator:prey size ratios, because the larger

phytoplankton are heavily controlled by grazing and can only increase when there is enough zooplankton biomass to support the largest (omnivorous) predators. We do not see such results in our models, perhaps because of the differences in feeding kernel. Fuchs & Franks (2010) also saw a noticeable flattening of the spectral slopes with increased nutrients, unlike the results in our model.

Also in the Fuchs & Franks (2010) model, as the width of the feeding kernel increased (i.e. the predators are more generalists), the spectra became steeper and more non-linear. In Banas (2011), increased generality of grazing led to peaks and valleys in size spectra. In Chang et al. (2014), increased omnivory and activity of the microbial food web led to curves in the size spectra due to smaller-sized consumers having a higher trophic level than larger organisms.

While our model results did not include discontinuities and distinctly domed size spectra, the inclusion of omnivory in Model 3 did lead to nonlinearities in the size distributions (Figs. 4 & 5). In our Model 3, omnivory, as might be expected, led to a decreased abundance of microzooplankton relative to the spectra of herbivorous microzooplankton (Models 1 & 2) (Fig. 5). Consequently, the phytoplankton threshold increased, allowing a greater abundance of phytoplankton relative to the herbivorous models (Fig. 4). However, this increase was limited to the smallest size classes, because, as stated above, the larger microzooplankton have higher grazing rates than smaller grazers at lower prey concentrations. Thus, the largest size classes of phytoplankton become depressed, as do the microzooplankton, due to their predation upon each other. Therefore, the inclusion of omnivory did lead to changes in the size spectra, but the changes were subtler than changes in nutrient regimes.

The comparison of our models with results from other size-structured models highlights other areas of pursuit. In particular, varying the predator:prey size ratio, size classes grazed by omnivores, and shape of the feeding kernel within the models presented here may lead to interesting dynamics, generating useful insights into the structuring of planktonic ecosystems. While beyond the scope of this study, we recommend these ideas as potential areas of interest for future studies.

Planktonic spectral slopes

Given that the 3 models generated similar planktonic community structures, it is instructive to examine the dynamics that determine the different spectral slopes. We can explore this quantitatively from the analytical solutions of Model 1 (see also Poulin & Franks 2010) using the new parameterizations of the model. We also emphasize that the method outlined below can be used to determine how different parameter values may alter the emergent community size structure.

From Model 1, the value of P^* (the phytoplankton biomass of a given size class that exists at equilibrium) is given by

$$P^* = \frac{k_z}{\Gamma g/\Delta - 1} \tag{6}$$

which is Eq. (18) from Poulin & Franks (2010), modified to match the notation used in this study. Because phytoplankton biomass in a given size class is on the order of 0.01 µmol N l^{-1} and k_z is on the order of 10 to 0.1 µmol N l^{-1}, at steady state the grazing can be assumed to be linear. Thus, Eq. (6) simplifies to

$$P^* = \frac{k_z \Delta}{\Gamma g} = \frac{k_{z,0} s^{e_{kz}} \Delta_0 s^{e_\Delta}}{\Gamma_0 s^{e_\Gamma} g_0 s^{e_g}} \tag{7}$$

which is Eqs. (19) & (20) from Poulin & Franks (2010). In Eq. (7), the rightmost side corresponds to each variable being written out in its explicit size-dependent form according to the allometric relationship in Eq. (1). That is, an arbitrary parameter x can be described by its coefficient x_0, size s, and exponent e_x. For the phytoplankton, we put the values from Table 1 into Eq. (7) and simplify to yield

$$P^* = \frac{k_{z,0} s^{-0.64} \Delta_0 s^0}{\Gamma_0 s^0 g_0 s^{-0.66}} = \frac{k_{z,0} \Delta_0}{\Gamma_0 g_0} s^{0.02} \tag{8}$$

Subtracting 1 from the above exponent to take into account a spectrum normalized by the width of the size classes results in a slope of −0.98, almost identical to the phytoplankton spectral slopes obtained from all the models for all nutrient concentrations (Fig. 4, Table 2). This slope arises from the difference in the size dependencies of the grazing parameters g and k_z (Eq. 8); since they are of almost equal magnitude, the normalized spectrum has a slope close to −1. Thus the phytoplankton biomass spectrum is determined by the microzooplankton parameters: the amount of phytoplankton of a given size is determined by the grazing, which decreases the competitive advantage of the smallest phytoplankton, allowing the larger phytoplankton to grow.

To examine which parameters determine the microzooplankton spectral slope, we perform a similar process as above to calculate Z^*, the microzooplankton concentration at equilibrium. From Eq. (22) of Poulin & Franks (2010),

$$Z^{\star} = \left(\frac{P^{\star}+k_Z}{g}\right)\left(\mu\frac{N^{\star}}{N+k_s}-\Lambda\right) \quad (9)$$

To explore which parameters affect the microzooplankton spectral slope, we made a few simplifications to Eq. (9). First, we regard $N^{\star}$ as just N. Second, because k_s is on the order of 0.1 to 1 µmol N l^{-1} and N is on the order of 0.01 µmol N l^{-1}, nutrient uptake can be assumed to be linear. Recalling that grazing can also be assumed to be linear and adopting the notation of explicitly writing out the size dependencies of each variable, Eq. (9) simplifies to

$$Z^{\star} = \left(\frac{k_z}{g}\right)\left(\mu\frac{N}{k_s}-\Lambda\right) = \left(\frac{k_{z,0}s^{e_{kz}}}{g_0 s^{e_g}}\right)\left(\mu_0 s^{e_\mu}\frac{N}{k_{s,0}s^{e_{kz}}}-\Lambda_0 s^{e_\Lambda}\right) \quad (10)$$

Putting in the exponent values from Table 1 and simplifying, Eq. (10) becomes

$$Z^{\star} = \left(\frac{k_{z,0}s^{-0.64}}{g_0 s^{-0.66}}\right)\left(\mu_0 s^{-0.16}\frac{N}{k_{s,0}s^{0.48}}-\Lambda_0 s^{0}\right) = \left(\frac{k_{z,0}}{g_0}s^{0.02}\right)\left(\mu_0\frac{N}{k_{s,0}}s^{-0.64}-\Lambda_0\right) \quad (11)$$

Again, after subtracting 1 to account for the normalized biomass, the microzooplankton spectrum predicted from the analytical solution is ca. −1.64 (Table 2). Noting that the exponent in the first term in Eq. (11) is close to zero, the microzooplankton size–biomass slope is mostly governed by the difference of the size dependencies of the phytoplankton growth rate □ and their half-saturation constant k_s. The size spectrum of the microzooplankton is controlled by the growth rates of their phytoplanktonic prey: larger phytoplankton grow more slowly, supporting a lower relative biomass of large microzooplankton.

Overall, while the microzooplankton parameters determine the phytoplankton size distribution, the phytoplankton parameters largely govern the microzooplankton size spectrum. That is, the phytoplankton are top-down controlled, while the microzooplankton are under bottom-up control. While these analytical solutions were obtained explicitly for Model 1, because the frameworks for each model are the same and because the spectral slopes changed very little with grazing behavior, the same general results applied to Models 2 and 3. However, the overlap among size spectra from all models was not exact, and thus the trophic dynamics did have subtle affects on the community structure. For example, Model 3 gave slightly different results because, as described earlier (see the 'Modeled size distributions' subsection), the inclusion of omnivory releases phytoplankton from grazing pressure while increasing losses of microzooplankton, leading to interactions among size classes that alter the community structure.

Nevertheless, even with significant structural changes to the modeled ecosystems (specialist vs. generalist herbivores and the inclusion of generalist omnivory), the same basic processes govern the planktonic size dependencies: the growth rate of the phytoplankton determines the amount of microzooplankton that can be supported in a given size class, and the grazing rate of the microzooplankton controls the amount of phytoplankton of a given size. Thus the emergent structure of planktonic ecosystems is a function of the simultaneous top-down and bottom-up control and is a relatively robust feature even in the face of differing degrees of trophic complexity in the ecosystem.

Sensitivity analysis

It is useful to examine in more detail the dependence of the planktonic community structure on each of the model parameters. We did this through a sensitivity analysis that determines the change of phytoplankton and microzooplankton biomass given an increase or decrease in any one parameter. This analysis indicates which parameters are most influential in determining our emergent planktonic communities, and, consequently, which parameters must be known with the greatest confidence to obtain accurate size distributions. A more thorough analysis may include the sensitivity of the models to simultaneous changes in multiple parameters, but such an analysis can quickly become intractable when including several variables.

To perform the sensitivity analysis, we calculated the partial derivative of the steady-state microzooplankton and phytoplankton biomass with respect to the coefficient and exponent of each parameter. We chose this method because the partial derivative is one of the most fundamental sensitivity analyses (Hamby 1994). However, we have also restricted our analysis to Model 1 because that model forms the foundation for Models 2 and 3. Insight from Model 1, while not exact, can still shed light on the sensitivity of the parameters in the other models, given the similarity in results among modeled ecosystems (Figs. 4 & 5, Table 2).

We normalized the partial derivative by the reciprocal of the variables, making our sensitivity metric dimensionless and thus appropriate to compare among all parameters. For example, to calculate the

importance of the value of the grazing coefficient g_0 on the microzooplankton spectrum Z, we calculated $\frac{g_0}{Z}\frac{\partial Z}{\partial g_0}$, which is approximately equal to calculating a percent change in the dependent variable given a percent change in the independent variable or $\frac{\%\Delta Z}{\%\Delta g_0}$. Because these partial derivatives have the potential to be size-dependent, the percent changes are also size-specific, as will be highlighted below.

From Eq. (7) we found that the exponent for microzooplankton grazing e_g has the greatest potential effect on the phytoplankton spectral slope, especially for the largest size classes, closely followed by the exponent for k_z for the smallest size classes (Table 3). The maximum sensitivity value of 4.98 for e_g means that, for a 1% increase in e_g, the phytoplankton biomass for the largest size classes increases about 5%. Changing e_{kz} leads to a similar effect on phytoplankton, but the relationship is negative and affects the smallest size classes. That is, for a 1% increase in e_{kz}, the phytoplankton biomass decreases by approximately −4.8% among the smallest size classes. We do note, however, that because the phytoplankton biomass decreases with increasing size, a percent increase for the larger size classes is not as great an absolute change as for the smaller size classes.

Table 3. Sensitivity of phytoplanktonic size spectrum to non-zero parameters. Parameters with a 0 subscript indicate coefficients and *e* indicates the exponent for the parameter in the exponential subscript (e.g. $a = a_0 s^{e_a}$, where s = size). The max and min values are based on a size range from 0.8 µm to 1900 µm, i.e. the approximate size range produced in the models

Parameter	Equation	Sensitivity value	Min value	Max value
$k_{z,0}$	$\frac{k_{z,0}}{P^\star}\frac{\partial P^\star}{\partial k_{z,0}} = 1$	1	1	1
e_{kz}	$\frac{e_{kz}}{P^\star}\frac{\partial P^\star}{\partial e_{kz}} = e_{kz}\ln(s)$	$-0.64\ln(s)$	−4.83	0.14
g_0	$\frac{g_0}{P^\star}\frac{\partial P^\star}{\partial g_0} = -1$	−1	−1	−1
e_g	$\frac{e_g}{P^\star}\frac{\partial P^\star}{\partial e_g} = -e_g\ln(s)$	$0.66\ln(s)$	−0.15	4.98
Λ_0	$\frac{\Lambda_0}{P^\star}\frac{\partial P^\star}{\partial \Lambda_0} = 1$	1	1	1
Γ_0	$\frac{\Gamma_0}{P^\star}\frac{\partial P^\star}{\partial \Gamma_0} = -1$	−1	−1	−1

For the remaining variables, the phytoplankton biomass varied by a constant amount. That is, for a given percent change in a parameter, the phytoplankton biomass for each size class varied by the same percent. This relationship can be positive, as for the coefficients for k_z and Λ, or negative, as for the coefficients for g and Γ.

The most influential parameter determining the microzooplankton spectral slope is by far the exponent for the maximum grazing rate: e_g. The value of ~500 can be interpreted as a 1% change in e_g results in a 500% change in the largest microzooplankton size classes. Although this value may seem quite large, we point out that the microzooplankton spectrum for Model 1 decreases sharply for the larger size classes, so the absolute change in biomass is actually quite small. The next most influential parameter for the microzooplankton biomass is the exponent for the grazing half-saturation constant e_{kz}, which decreased the microzooplankton biomass by ~4.5% for the smallest size classes, which, again we point out, are much more abundant than the largest size classes. The remaining parameters influence the microzooplankton biomass by 2 to 0.002% (Table 4).

This exercise clearly shows how varying the allometric scalings of any of the parameters will affect either planktonic size distribution. In particular, both the phytoplankton and microzooplankton are most sensitive to the exponent for the maximum grazing rate. Therefore, knowledge of this parameter is the most important to obtain accurate estimates of planktonic biomass.

Because Models 2 and 3 with herbivorous and omnivorous grazing on multiple size classes of plankton have the same model framework as Model 1, the latter model's sensitivity analysis can provide some insight into the other models. The inclusion of generalist grazers (Model 2) did not lead to large changes in planktonic biomass for most size classes. However, the decrease in microzooplankton biomass among the smallest sizes in Model 2 (Fig. 5) indicates that this increasing feeding complexity can lead to some changes in community structure, as may be expected given the sensitivity of planktonic biomass to changes in g. The expanded feeding range of microzooplankton in this model creates more competition for the abundant phytoplankton size classes. This increased competition among microzooplankton was associated with a decrease in microzooplankton biomass at the small (abundant) end of the size spectrum where the lack of even smaller size classes forces intensified grazing on the smallest classes of phytoplankton.

Table 4. Sensitivity of zooplanktonic size spectrum to non-zero parameters. The parameters are in the same form as in Table 3. The max and min values are based on a size range from 0.8 µm to 1900 µm, i.e. the approximate size range produced in the models

Parameter	Equation	Sensitivity value	Min value	Max value
$k_{z,0}$	$\frac{k_{z,0}}{Z^*}\frac{\partial Z^*}{\partial k_{z,0}} = 1$	1	1	1
e_{kz}	$\frac{e_{kz}}{Z^*}\frac{\partial Z^*}{\partial e_{kz}} = e_{kz}\ln(s)$	$-0.64\ln(s)$	−4.46	0.14
g_0	$\frac{g_0}{Z^*}\frac{\partial Z^*}{\partial g_0} = \frac{-2\Delta_0 - \Gamma_0 g_0 s^{e_g}}{\Delta_0 + \Gamma_0 g_0 s^{e_g}}$	$\frac{-0.05-10.87s^{-0.66}}{0.025+10.87s^{-0.66}}$	−1.25	−1.00
e_g	$\frac{e_g}{Z^*}\frac{\partial Z^*}{\partial e_g} = \frac{-2\Delta_0 e_g \ln(s) - \Gamma_0 g_0 s^{e_g} e_g \ln(s)}{\Delta_0 + \Gamma_0 g_0 s^{e_g}}$	$\frac{6.84\ln(s)}{0.025+10.87s^{-0.66}}$	−0.12	518.90
Δ_0	$\frac{\Delta_0}{Z^*}\frac{\partial Z^*}{\partial \Delta_0} = \frac{\Delta_0}{\Delta_0 + \Gamma_0 g_0 s^{e_g}}$	$\frac{0.025}{0.025+10.87s^{-0.66}}$	0.002	0.25
Γ_0	$\frac{\Gamma_0}{Z^*}\frac{\partial Z^*}{\partial \Gamma_0} = \frac{-\Delta_0\Gamma_0 g_0 s^{e_g}}{\Delta_0 + \Gamma_0 g_0 s^{e_g}}$	$\frac{0.27s^{-0.66}}{0.025+10.87s^{-0.66}}$	0.02	0.25
Λ_0	$\frac{\Lambda_0}{Z^*}\frac{\partial Z^*}{\partial \Lambda_0} = \frac{2\mu_0 s^{e_\mu} + \Lambda_0}{\mu_0 s^{e_\mu} + \Lambda_0}$	$\frac{2.72s^{-0.16}+0.0015}{1.36s^{-0.16}+0.0015}$	2.00	2.00
□$_0$	$\frac{\mu_0}{Z^*}\frac{\partial Z^*}{\partial \mu_0} = \frac{-\mu_0 s^{e_\mu}}{\Lambda_0 + \mu_0 s^{e_\mu}}$	$\frac{-1.36.s^{-0.16}}{0.0015+1.36s^{-0.16}}$	−1.00	−1.00
$e_□$	$\frac{-e_\mu}{Z^*}\frac{\partial Z^*}{\partial e_\mu} = \frac{-e_\mu\mu_0 s^{e_\mu}\ln(s)}{\Lambda_0 + \mu_0 s^{e_\mu}}$	$\frac{-0.22s^{-0.16}\ln(s)}{0.0015+1.36s^{-0.16}}$	−1.22	0.036

With the inclusion of omnivory (Model 3), the spectral patterns and dependence on nutrient concentration changed compared to the other models. These changes were expected, based on the sensitivity analysis showing the strong dependency of the community structure on the grazing parameters. Here, omnivory tended to decrease the diversity of planktonic communities, as seen by the steep drop in large phytoplankton biomass and the decrease in phytoplankton spectral slope at each total nutrient concentration (Fig. 4). Ho et al. (2013) examined the influence of omnivorous feeding breadth and nutrient concentrations on planktonic size spectra and found that diversity decreased, i.e. whole planktonic size classes became extinct, both under high and low nutrient influx conditions when the feeding breadth was small. However, they also found an increase in top predators with strong omnivorous feeding, which is dissimilar from our model in which microzooplankton biomass decreased with omnivory. Nevertheless, their model only contained 3 size classes of microzooplankton and 1 of phytoplankton, limiting the interaction among size classes and thus the patterns that may emerge with higher size resolution.

CONCLUSION

In this study, we used a modeling framework to examine the influence of the size dependence of physiological rates, trophic dynamics, and nutrient regime on the emergent size structuring of planktonic communities. In our parameterization of physiological rates, we determined the allometric scalings of fundamental processes affecting phytoplankton and microzooplankton growth and grazing. However, phytoplankton and microzooplankton mortality were parameterized as constants for all size classes due to the scarcity of mortality rates in the literature. We hope that future studies will help determine these rates for a wider size range and variety of organisms to better determine their allometric scalings for use in future models. We also use a simplified, monotonic decrease in maximum phytoplankton growth rate with increasing size but hope to use more complex patterns in future studies.

Using our parameterizations, we examined the effect of trophic dynamics by increasing the complexity of microzooplankton feeding behavior in successive models. Overall, the more complex feeding

behavior had little influence on the size distribution of either the phytoplankton or microzooplankton. However, there were some subtle changes, such as the greater control of the most abundant size classes with the introduction of herbivorous feeding on multiple size classes and the increase in the small phytoplankton biomass and subsequent decrease in microzooplankton biomass with the inclusion of omnivorous grazing on multiple size classes of plankton. In contrast to these variations, increasing the total nutrient concentration had the noticeable and consistent effect of increasing the proportion of large plankton relative to small plankton, a feature often seen in the field. This increase occurred consistently through the addition of larger plankton in more nutrient-rich systems, rather than a change in the slope of the size spectra.

Another common quality of natural planktonic communities is the decrease in normalized biomass with increasing size. All combinations of grazing complexity and total nutrient concentrations were able to reproduce the negative normalized biomass spectral slopes. This general spectral shape for each planktonic group is largely determined by the rates of the other planktonic type. That is, the microzooplankton spectral slope is chiefly governed by the bottom-up control of the phytoplankton, and the phytoplankton spectrum is determined by the top-down forcing of the microzooplankton parameters. From our sensitivity analysis, we found that the exponent for the maximum microzooplankton grazing rate had the most influence on both the phyto- and microzooplankton biomass. Therefore, this parameter should be known with the greatest amount of certainty because changes in this parameter lead to the largest variance in planktonic biomass.

Acknowledgements. F.J.P. thanks NSERC for financial support during this work. We thank Mike Landry for his significant contribution. We also thank the reviewers for their constructive comments in improving this work.

LITERATURE CITED

Aelion CM, Chisholm SW (1985) Effect of temperature on growth and ingestion rates of *Favella* sp. J Plankton Res 7:821–830

Agusti S, Satta MP, Mura MP, Benavent E (1998) Dissolved esterase activity as a tracer of phytoplankton lysis: evidence of high phytoplankton lysis rates in the northwestern Mediterranean. Limnol Oceanogr 43:1836–1849

Ahrens MA, Peters RH (1991) Patterns and limitations in limnoplankton size spectra. Can J Fish Aquat Sci 48: 1967–1978

Armstrong RA (1994) Grazing limitation and nutrient limitation in marine ecosystems: steady state solutions of an ecosystem model with multiple food chains. Limnol Oceanogr 39:597–608

Banas NS (2011) Adding complex trophic interactions to a size-spectral plankton model: emergent diversity patterns and limits on predictability. Ecol Model 222: 2663–2675

Banse K (1976) Rates of growth, respiration and photosynthesis of unicellular algae as related to cell-size—a review. J Phycol 12:135–140

Banse K (1982) Cell volumes, maximal growth rates of unicellular algae and ciliates, and the role of ciliates in the marine pelagial. Limnol Oceanogr 27:1059–1071

Bec B, Collos Y, Vaquer A, Mouillot D, Souchu P (2008) Growth rate peaks at intermediate cell size in marine photosynthetic picoeukaryotes. Limnol Oceanogr 53: 863–867

Bidle KD, Falkowski PG (2004) Cell death in planktonic, photosynthetic microorganisms. Nat Rev Microbiol 2: 643–655

Borsheim KY, Bratbak G (1987) Cell volume to cell carbon conversion factors for a bactivorous *Monas* sp. enriched from seawater. Mar Ecol Prog Ser 36:171–175

Brown JH, Gillooly JF, Allen AP, Savage VM, West GB (2004) Toward a metabolic theory of ecology. Ecology 85: 1771–1789

Brussaard CPD (2004) Viral control of phytoplankton populations—a review. J Eukaryot Microbiol 51:125–138

Brussaard CPD, Riegman R, Noordeloos AAM, Cadee GC and others (1995) Effects of grazing, sedimentation and phytoplankton cell lysis on the structure of a coastal pelagic food web. Mar Ecol Prog Ser 123:259–271

Brussaard CPD, Gast GJ, vanDuyl FC, Riegman R (1996) Impact of phytoplankton bloom magnitude on a pelagic microbial food web. Mar Ecol Prog Ser 144:211–221

Button DK (1978) On the theory of control of microbial growth kinetics by limiting nutrient concentrations. Deep-Sea Res 25:1163–1177

Calbet A, Landry MR (2004) Phytoplankton growth, microzooplankton grazing, and carbon cycling in marine systems. Limnol Oceanogr 49:51–57

Caron DA, Goldman JC, Dennett MR (1986) Effect of temperature on growth, respiration, and nutrient regeneration by an omnivorous microflagellate. Appl Environ Microbiol 52:1340–1347

Cavender-Bares KK, Rinaldo A, Chisholm SW (2001) Microbial size spectra from natural and nutrient enriched ecosystems. Limnol Oceanogr 46:778–789

Chan AT (1978) Comparative physiological study of marine diatoms and dinoflagellates in relation to irradiance and cell size. 1. Growth under continuous light. J Phycol 14: 396–402

Chang CW, Takeshi M, Shiah FK, Kao S, Wu JT, Sastri AR, Hsieh CH (2014) Linking secondary structure of individual size distribution with nonlinear size–trophic level relationship in food webs. Ecology 95:897–909

Chang FH, Marquis EC, Chang CW, Gong GC, Hsieh CH (2013) Scaling of growth rate and mortality with size and its consequence on size spectra of natural microphytoplankton assemblages in the East China Sea. Biogeosciences 10:5267–5280

Chen B, Landry MR, Huang B, Liu H (2012) Does warming enhance the effect of microzooplankton grazing on marine phytoplankton in the ocean? Limnol Oceanogr 57: 519–526

Chisholm SW (1992) Phytoplankton size. In: Falkowski PG, Woodhead AD (eds) Primary productivity and biogeochemical cycles in the sea. Plenum Press, New York, NY, p 213–237

Choi JW, Peters F (1992) Effects of temperature on psychrophilic ecotypes of a heterotrophic nanoflagellate, *Paraphysomonas imperforata*. Appl Environ Microbiol 58:593–599

Cottrell MT, Suttle CA (1995) Dynamics of a lytic virus infecting the photosynthetic marine picoflagellate *Micromonas pusilla*. Limnol Oceanogr 40:730–739

DeLong JP, Okie JG, Moses ME, Sibly RM, Brown JH (2010) Shifts in metabolic scaling, production, and efficiency across major evolutionary transitions of life. Proc Natl Acad Sci USA 107:12941–12945

Edwards KF, Thomas MK, Klausmeier CA, Litchman E (2012) Allometric scaling and taxonomic variation in nutrient utilization traits and maximum growth rate of phytoplankton. Limnol Oceanogr 57:554–566

Eppley RW (1972) Temperature and phytoplankton growth in the sea. Fish Bull 70:1063–1085

Eppley RW, Sloan PR (1966) Growth rates of marine phytoplankton: correlation with light absortpion by cell chlorophyll *a*. Physiol Plant 19:47–59

Eppley RW, Rogers JN, McCarthy JJ (1969) Half-saturation constants for uptake of nitrate and ammonium by marine phytoplankton. Limnol Oceanogr 14:912–920

Fenchel T (1974) Intrinsic rate of natural increase: relationship with body size. Oecologia 14:317–326

Fenchel T (1980) Suspension feeding in ciliated protozoa: feeding rates and their ecological significance. Microb Ecol 6:13–25

Fenchel T, Finlay BJ (1983) Respiration rates in heterotrophic free-living protozoa. Microb Ecol 9:99–122

Finkel ZV (ed) (2007) Does phytoplankton cell size matter? The evolution of modern marine food webs. In: Falkowski PG, Knoll AH (eds) Evolution of primary producers in the sea. Elsevier Academic Press, Burlington, MA, p 333–350

Finkel ZV, Irwin AJ (2000) Modeling size-dependent photosynthesis: light absorption and the allometric rule. J Theor Biol 204:361–369

Finkel ZV, Irwin AJ, Schofield O (2004) Resource limitation alters the 3/4 size scaling of metabolic rates in phytoplankton. Mar Ecol Prog Ser 273:269–279

Fischer MG, Allen MJ, Wilson WH, Suttle CA (2010) Giant virus with a remarkable complement of genes infects marine zooplankton. Proc Natl Acad Sci USA 107:19508–19513

Franks PJS, Jaffe JS (2008) Microscale variability in the distributions of large fluorescent particles observed in situ with a planar laser imaging fluorometer. J Mar Syst 69: 254–270

Franks PJS, Wroblewski JS, Flierl GR (1986) Behavior of a simple plankton model with food-level acclimation by herbivores. Mar Biol 91:121–129

Fuchs HL, Franks PJS (2010) Plankton community properties determined by nutrients and size-selective feeding. Mar Ecol Prog Ser 413:1–15

Garza DR, Suttle CA (1995) Large double-stranded DNA viruses which cause the lysis of a marine heterotrophic nanoflagellate (*Bodo* sp.) occur in natural marine viral communities. Aquat Microb Ecol 9:203–210

Gentleman WC, Neuheimer AB (2008) Functional responses and ecosystem dynamics: how clearance rates explain the influence of satiation, food-limitation and acclimation. J Plankton Res 30:1215–1231

Gentleman W, Leising A, Frost B, Strom S, Murray J (2003) Functional responses for zooplankton feeding on multiple resources: a review of assumptions and biological dynamics. Deep-Sea Res II 50:2847–2875

Gin KYH, Chisholm SW, Olson RJ (1999) Seasonal and depth variation in microbial size spectra at the Bermuda Atlantic time series station. Deep-Sea Res I 46:1221–1245

Goericke R (2011) The size structure of marine phytoplankton - what are the rules? Calif Coop Ocean Fish Invest Rep 52:198–204

Gould SJ (1966) Allometry and size in ontogeny and phylogeny. Biol Rev Camb Philos Soc 41:587–640

Hamby DM (1994) A review of techniques for parameter sensitivity analysis of environmental models. Environ Monit Assess 32:135–154

Hansen B, Bjornsen PK, Hansen PJ (1994) The size ratio between planktonic predators and their prey. Limnol Oceanogr 39:395–403

Hansen PJ, Bjornsen PK, Hansen BW (1997) Zooplankton grazing and growth: scaling within the 2-2,000-µm body size range. Limnol Oceanogr 42:687–704

Healey FP (1980) Slope of the Monod equation as an indicator of advantage in nutrient competition. Microb Ecol 5: 281–286

Ho PC, Chang CW, Hsieh CH, Shiah FK, Miki T (2013) Effects of increasing nutrient supply and omnivorous feeding on the size spectrum slope: a size-based nutrient-phytoplankton-zooplankton model. Popul Ecol 55: 247–259

Irwin AJ, Finkel ZV, Schofield OME, Falkowski PG (2006) Scaling-up from nutrient physiology to the size-structure of phytoplankton communities. J Plankton Res 28: 459–471

Kempes CP, Dutkiewicz S, Follows MJ (2012) Growth, metabolic partitioning, and the size of microorganisms. Proc Natl Acad Sci USA 109:495–500

Kerr SR (1974) Theory of size distribution in ecological communities. J Fish Res Board Can 31:1859–1862

Landry MR (2002) Integrating classical and microbial food web concepts: evolving views from the open-ocean tropical Pacific. Hydrobiologia 480:29–39

Litchman E, Klausmeier CA, Schofield OM, Falkowski PG (2007) The role of functional traits and trade-offs in structuring phytoplankton communities: scaling from cellular to ecosystem level. Ecol Lett 10:1170–1181

Marañón E, Cermeno P, Rodriguez J, Zubkov MV, Harris RP (2007) Scaling of phytoplankton photosynthesis and cell size in the ocean. Limnol Oceanogr 52:2190–2198

Marañón E, Cermeno P, Lopez-Sandoval DC, Rodriguez-Ramos T and others (2013) Unimodal size scaling of phytoplankton growth and the size dependence of nutrient uptake and use. Ecol Lett 16:371–379

Massana R, del Campo J, Dinter C, Sommaruga R (2007) Crash of a population of the marine heterotrophic flagellate *Cafeteria roenbergensis* by viral infection. Environ Microbiol 9:2660–2669

Menden-Deuer S, Lessard EJ (2000) Carbon to volume relationships for dinoflagellates, diatoms, and other protist plankton. Limnol Oceanogr 45:569–579

Mizuno M (1991) Influence of cell volume on the growth and size reduction of marine and estuarine diatoms. J Phycol 27:473–478

Moloney CL, Field JG (1989) General allometric equations for rates of nutrient uptake, ingestion, and respiration in plankton organisms. Limnol Oceanogr 34:1290–1299

Moloney CL, Field JG (1991) The size-based dynamics of plankton food webs. 1. A simulation model of carbon and nitrogen flows. J Plankton Res 13:1003–1038

Nagasaki K, Ando M, Imai I, Itakura S, Ishida Y (1993) Virus-like particles in an apochlorotic flagellate in Hiroshima Bay, Japan. Mar Ecol Prog Ser 96:307–310

Peters F (1994) Prediction of planktonic protistan grazing rates. Limnol Oceanogr 39:195–206

Platt T, Denman K (1977) Organization in the pelagic ecosystem. Helgol Wiss Meeresunters 30:575–581

Platt T, Denman K (1978) The structure of pelagic marine ecosystems. Rapp PV Reùn Cons Int Explor Mer 173:60–65

Poulin FJ, Franks PJS (2010) Size-structured planktonic ecosystems: constraints, controls and assembly instructions. J Plankton Res 32:1121–1130

Raimbault P, Rodier M, Taupier-Letage I (1988) Size fraction of phytoplankton in the Ligurian Sea and the Algerian Basin (Mediterranean Sea): size distribution versus total concentration. Mar Microb Food Webs 3:1–8

Reul A, Rodriguez V, Jimenez-Gomez F, Blanco JM and others (2005) Variability in the spatio-temporal distribution and size-structure of phytoplankton across an upwelling area in the NW-Alboran Sea, (W-Mediterranean). Cont Shelf Res 25:589–608

Reul A, Rodriguez J, Guerrero F, Gonzalez N and others (2008) Distribution and size biomass structure of nanophytoplankton in the Strait of Gibraltar. Aquat Microb Ecol 52:253–262

Riegman R, van Bleijswijk JDL, Brussaard CPD (2002) The use of dissolved esterase activity as a tracer of phytoplankton lysis — Comment. Limnol Oceanogr 47:916–920

Rodriguez J, Mullin MM (1986) Relation between biomass and body weight of plankton in a steady-state oceanic ecosystem. Limnol Oceanogr 31:361–370

San Martin E, Harris RP, Irigoien X (2006) Latitudinal variation in plankton size spectra in the Atlantic Ocean. Deep-Sea Res II 53:1560–1572

Saura A, Massana R, Boras JA, Forn I, Vila-Reixach G, Vaque D (2011) Effect of viruses on marine stramenopile (MAST) communities in an oligotrophic coastal marine system. J Plankton Res 33:1709–1718

Sheldon RW, Prakash A, Sutcliffe WH (1972) The size distribution of particles in the ocean. Limnol Oceanogr 17: 327–340

Sheldon RW, Sutcliffe WH, Paranjape MA (1977) Structure of pelagic food chain and relationship between plankton and fish production. J Fish Res Board Can 34:2344–2353

Sommer U (1989) Maximal growth rates of Antarctic phytoplankton: only weak depenence on cell size. Limnol Oceanogr 34:1109–1112

Sprules WG, Munawar M (1986) Plankton size spectra in relation to ecosystem productivity, size, and perturbation. Can J Fish Aquat Sci 43:1789–1794

Steele JH, Frost BW (1977) The structure of plankton communities. Philos Trans R Soc Lond B Biol Sci 280:485–534

Stock CA, Powell TM, Levin SA (2008) Bottom-up and top-down forcing in a simple size-structured plankton dynamics model. J Mar Syst 74:134–152

Straile D (1997) Gross growth efficiencies of protozoan and metazoan zooplankton and their dependence on food concentration, predator-prey weight ratio, and taxonomic group. Limnol Oceanogr 42:1375–1385

Suttle CA, Chan AM (1994) Dynamics and distribution of cyanophages and their effect on marine *Synechococcus* spp. Appl Environ Microbiol 60:3167–3174

Tang EPY (1995) The allometry of algal growth rates. J Plankton Res 17:1325–1335

Tang EPY, Peters RH (1995) The allometry of algal respiration. J Plankton Res 17:303–315

Thingstad TF (1998) A theoretical approach to structuring mechanisms in the pelagic food web. Hydrobiologia 363: 59–72

Tilman D, Hillerislambers J, Harpole S, Dybzinski R, Fargione J, Clark C, Lehman C (2004) Does metabolic theory apply to community ecology? It's a matter of scale. Ecology 85:1797–1799

Uitz J, Claustre H, Morel A, Hooker SB (2006) Vertical distribution of phytoplankton communities in open ocean: an assessment based on surface chlorophyll. J Geophys Res 111:C08005

van Boekel WHM, Hansen FC, Riegman R, Bak RPM (1992) Lysis-induced decline of a *Phaeocystis* spring bloom and coupling with the microbial foodweb. Mar Ecol Prog Ser 81:269–276

Verity PG (1985) Grazing, respiration, excretion, and growth rates of tintinnids. Limnol Oceanogr 30:1268–1282

Ward BA, Dutkiewicz S, Jahn O, Follows MJ (2012) A size-structured food-web model for the global ocean. Limnol Oceanogr 57:1877–1891

Weinbauer MG, Hofle MG (1998) Size-specific mortality of lake bacterioplankton by natural virus communities. Aquat Microb Ecol 15:103–113

Williams RB (1964) Division rates of salt marsh diatoms in relation to salinity and cell size. Ecology 45:877–880

Zarauz L, Irigoien X, Fernandes JA (2009) Changes in plankton size structure and composition, during the generation of a phytoplankton bloom, in the central Cantabrian sea. J Plankton Res 31:193–207

Editorial responsibility: Edward Durbin, Narragansett, Rhode Island, USA

Submitted: December 11, 2013; Accepted: July 23, 2014
Proofs received from author(s): October 10, 2014